Nonsyndromic Retinal Dystrophy due to Bi-Allelic Mutations in the Ciliary Transport Gene *IFT140*

Sarah Hull,[1,2] Nicholas Owen,[1] Farrah Islam,[2,3] Dhani Tracey-White,[1] Vincent Plagnol,[4] Graham E. Holder,[1,2] Michel Michaelides,[1,2] Keren Carss,[5,6] F. Lucy Raymond,[6,7] Jean-Michel Rozet,[8] Simon C. Ramsden,[9] Graeme C. M. Black,[9,10] Isabelle Perrault,[8] Ajoy Sarkar,[11] Mariya Moosajee,[1,2] Andrew R. Webster,[1,2] Gavin Arno,[1,2] and Anthony T. Moore[1,2,12]

[1]University College London Institute of Ophthalmology, London, United Kingdom
[2]Moorfields Eye Hospital, London, United Kingdom
[3]Al-Shifa Trust Eye Hospital, Rawalpindi, Pakistan
[4]University College London Genetics Institute, London, United Kingdom
[5]Department of Haematology, University of Cambridge, Cambridge, United Kingdom
[6]NIHR BioResource—Rare Diseases, Department of Haematology, University of Cambridge, Cambridge, United Kingdom
[7]Department of Medical Genetics, Cambridge Institute for Medical Research, University of Cambridge, Cambridge, United Kingdom
[8]Laboratory of Genetics in Ophthalmology, INSERM UMR 1163, Paris Descartes-Sorbonne University, Imagine Institut, Paris, France
[9]Manchester Centre for Genomic Medicine, Central Manchester University Hospitals NHS Foundation Trust, Manchester Academic Health Sciences Centre, St Mary's Hospital, Manchester, United Kingdom
[10]Manchester Centre for Genomic Medicine, Institute of Human Development, Faculty of Medical and Human Sciences, University of Manchester, Manchester, United Kingdom
[11]Department of Clinical Genetics, Nottingham City Hospital, Nottingham, United Kingdom
[12]Ophthalmology, University of California, San Francisco, California, United States

Correspondence: Anthony T. Moore, Professorial Unit, Moorfields Eye Hospital NHS Trust, 162 City Road, London EC1V 2PD, UK; tony.moore@ucl.ac.uk.
Gavin Arno; g.arno@ucl.ac.uk.

Submitted: August 17, 2015
Accepted: January 12, 2016

Citation: Hull S, Owen N, Islam F, et al. Nonsyndromic retinal dystrophy due to bi-allelic mutations in the ciliary transport gene *IFT140*. *Invest Ophthalmol Vis Sci*. 2016;57:1053–1062. DOI:10.1167/iovs.15-17976

Purpose. Mutations in the ciliary transporter gene *IFT140,* usually associated with a severe syndromic ciliopathy, may also cause isolated retinal dystrophy. A series of patients with nonsyndromic retinitis pigmentosa (RP) due to *IFT140* was investigated in this study.

Methods. Five probands and available affected family members underwent detailed phenotyping including retinal imaging and electrophysiology. Whole exome sequencing was performed on two probands, a targeted sequencing panel of 176 retinal genes on a further two, and whole genome sequencing on the fifth. Missense mutations of *IFT140* were further investigated in vitro using transient plasmid transfection of hTERT-RPE1 cells.

Results. Eight affected patients from five families had preserved visual acuity until at least the second decade; all had normal development without skeletal manifestations or renal failure at age 13 to 67 years (mean, 42 years; median, 44.5 years). Bi-allelic mutations in *IFT140* were identified in all families including two novel mutations: c.2815T > C (p.Ser939Pro) and c.1422_23insAA (p.Arg475Asnfs*14). Expression studies demonstrated a significantly reduced number of cells showing localization of mutant IFT140 with the basal body for two nonsyndromic mutations and two syndromic mutations compared with the wild type and a polymorphism.

Conclusions. This study highlights the phenotype of nonsyndromic RP due to mutations in *IFT140* with milder retinal dystrophy than that associated with the syndromic disease.

Keywords: retinitis pigmentosa, ciliopathy, next-generation sequencing

The outer segments of photoreceptors are highly modified, photosensitive cilia, which lack any capability for protein production.[1] Thus, they are reliant on the intraflagellar transport (IFT) system, which comprises large protein complexes for transport from the cell body to cilium tip and back driven by the motors kinesin-2 and dynein-2, respectively.[2] The IFT-B complex is essential for cilium assembly and anterograde transport, whereas the IFT-A complex is responsible for retrograde transport, with additional roles in anterograde transport by connecting kinesin to the IFT complex and in facilitating entry of proteins in to the cilium.[3,4] IFT140, a subunit of IFT-A, is vital for both the development and the maintenance of outer segments and has a specific role in opsin transport across the connecting cilium.[2]

Mutations in *IFT140* have been associated with Jeune asphyxiating thoracic dystrophy and Mainzer-Saldino syndrome, ciliopathies forming part of a spectrum of skeletal dysplasias now collectively termed short rib thoracic dysplasia 9 with or without polydactyly (SRTD9, mendelian inheritance in man [MIM]#266920).[5–7] First described in 1970, patients have variable skeletal features including shortened ribs, short stature, cone-shaped phalangeal epiphyses (prepubertal), brachymesophalangy, and acetabular spurring or metaphyseal defect of the femoral head.[8] Nonskeletal features in the

majority of patients include a severe early-onset retinal dystrophy and end-stage renal failure secondary to nephronophthisis by the teenage years, with cerebellar ataxia, epilepsy, facial dysmorphism, learning difficulties, and cholestasis also reported.[5–7]

Retinitis pigmentosa (RP) is the most common form of inherited retinal dystrophy, with more than 60 genes associated with the nonsyndromic, recessive form.[9–12] These include ciliopathy genes such as *CEP290* and *BBS1,* which manifest both syndromic and nonsyndromic phenotypes.[13,14] Recently, *IFT140* mutations have been identified in patients with isolated retinal dystrophy.[15,16] The present study reports eight patients from five families with isolated retinal dystrophy and bi-allelic *IFT140* variants with detailed characterization of the ocular phenotype. Functional analysis of two of these variants with protein localization studies in hTERT-RPE1 cells supports their pathogenicity.

Materials and Methods

The study protocol adhered to the tenets of the Declaration of Helsinki and received approval from the local ethics committees. Written informed consent was obtained from all participants prior to their inclusion in this study, with parental written consent provided on behalf of the children involved in this study.

Clinical Evaluation

Each proband with *IFT140*-related retinal dystrophy and available affected family members underwent a full clinical examination including visual acuity and dilated fundus examination. Retinal fundus imaging was obtained by conventional 35° fundus color photographs (Topcon Great Britain, Ltd., Berkshire, UK), fundus autofluorescence (FAF) imaging using 30° or 55° Spectralis (Heidelberg Engineering, Ltd., Heidelberg, Germany) or ultra-widefield confocal scanning laser imaging (Optos plc, Dunfermline, UK), and either Stratus optical coherence tomography (OCT; Carl Zeiss Meditec, Inc., Dublin, CA, USA) or Spectralis OCT (Heidelberg Engineering Ltd.). Full field and pattern electroretinography were performed using gold foil electrodes to incorporate the International Society for Clinical Electrophysiology of Vision (ISCEV) standards.[17,18] Renal function was performed in all available patients, with skeletal x-rays in five patients.

Molecular Investigations

Genomic DNA was isolated from peripheral blood lymphocytes using the Puregene kit (Gentra Puregene Blood Extraction Kit, Qiagen, Manchester, UK).

Patient 1.1 was initially negative for known retinal dystrophy variants using an arrayed primer extension (APEX)-based test (Asper Biotech, Ltd., Tartu, Estonia) using a genotyping microarray containing >300 disease causing variants and common polymorphisms for eight retinal dystrophy genes (*AIPL1, CRB1*, *CRX*, *GUCY2D*, *RPE65*, *RPGRIP1*, *LRAT*, and *MERTK*) as previously described.[19] He was then found negative by targeted next-generation sequencing (NGS) of the coding regions of 31 retinal dystrophy genes performed at the Bioscientia Center for Human Genetics (Ingelheim, Germany) using the Genome Sequencer FLX system (Roche, Basel, Switzerland), enriched using a Roche/NimbleGen sequence capture and analyzed using Roche GS Reference Mapper (version 2.5.3) and JSI Medical Systems Software (version 3.5; Ettenheim, Germany). Whole exome sequencing (WES) was performed at AROS Applied Biotechnology using a solution-phase Agilent SureSelect 38-Mb exome capture (SureSelect Human All Exon Kit; Agilent Technologies, Inc., Santa Clara, CA, USA) and the Illumina HiSeq 2000 sequencer (Illumina, Inc., San Diego, CA, USA). Reads were aligned to the hg19 human reference sequence using Novoalign (Novocraft, Selangor, Malaysia), version 2.05. The ANNOVAR tool (Openbioinformatics.org) was used to annotate single nucleotide polymorphisms (SNPs) and small insertions/deletions.

Patient 2 was initially investigated as part of the UK National Collaborative Usher study due to the coexistence of hearing loss with retinal dystrophy with negative bi-directional Sanger sequencing of nine Usher genes (*MYO7A, CDH23, PCDH15, USH1C, USH1G, USH2A, GPR98, WHRN,* and *CLRN1*) and a candidate gene *SLC4A7* as previously described.[20] WES was then performed as above.

Patients 3.1 and 5 underwent NGS of the coding regions of 176 retinal genes at the Manchester Centre for Genomic Medicine (Manchester, UK) with enrichment using a SureSelect Target Enrichment Kit (Agilent Technologies, Inc.) and then sequenced on the HiSeq 2500 (Illumina, Inc.). Sequenced reads were aligned to the human reference sequence hg19 (build GRCh37) with the Burrows-Wheeler aligner (BWA v0.6.2).[21] The genome analysis tool kit (GATKlite v2.0.39) was used for base quality score recalibration and indel realignment prior to variant calling using the UnifiedGenotyper.[22]

Patient 4 underwent whole genome sequencing (WGS) as part of the National Institute for Health Research (NIHR) BioResource- Rare Diseases study using the Illumina TruSeq DNA PCR-Free Sample preparation kit (Illumina, Inc.) and sequenced using an Illumina HiSeq 2500, generating minimum coverage of 15× for approximately 95% of the genome. Reads were aligned to the Genome Reference Consortium human genome build 37 (GRCh37) using Isaac Genome Alignment Software (version 01.14; Illumina, Inc.).[23] Single nucleotide variations and small insertion deletions were identified using Isaac Variant Caller (version 2.0.17).

Bi-directional Sanger sequencing of involved exons and intron-exon boundaries of *IFT140* was performed on all patients and segregation confirmed in available relatives. DNA was amplified using specifically designed primers by polymerase chain reaction (PCR), and the resulting fragments were sequenced using standard protocols (information on request).

Nomenclature was assigned in accordance with GenBank accession number NM_014714.3 with nucleotide position 1 corresponding to the A of the ATG translation initiation codon. Variants were identified as novel if not previously reported in the literature and if absent from dbSNP, which is available at http://www.ncbi.nlm.nih.gov/projects/SNP/, NHLBI GO Exome Sequencing Project (ESP; Seattle, WA, USA), which is available at http://evs.gs.washington.edu/EVS/, 1000 genomes project, which is available at http://www.1000genomes.org/, and the Exome aggregation Consortium (ExAC; Cambridge, MA, USA), which is available at http://exac.broadinstitute.org. All were accessed on November 25, 2015.[24] The likely pathogenicity of novel missense variants was assessed using the predictive algorithms of sorting intolerant from tolerant (SIFT), available at http://sift.jcvi.org, and polymorphism phenotyping v2 (PolyPhen-2), available at http://genetics.bwh.harvard.edu/pph2, and the conservation of the residues throughout the species was analyzed using Clustal Omega, accessed at http://www.ebi.ac.uk/Tools/msa/clustalo/, with protein sequences identified from Ensembl, which was accessed at http://www.ensembl.org.[25–28] Where relevant, potential splice site disruption was assessed using Splice Site Prediction by Neural Network at http://www.fruitfly.org/seq_tools/splice.html.[29]

Cell Transfection Studies

Site-directed mutagenesis using mutation-specific complementary primer pairs (Supplementary Table S1) generated four plasmid clones using pCMV-IFT140-Myc-DDK (RC207528; Origene, Rockville, MD, USA). Cultured hTERT-RPE1 cells were seeded at 1×10^5 cells/mL, and transient transfection was achieved using Lipofectamine LTX reagent with PLUS (Life Technologies, Paisley, UK). After incubation in OptiMEM-I reduced serum medium (Life Technologies) for 24 hours at 37°C in 5% CO_2, cells were fixated with 4% paraformaldehyde in PBS and then permeabilized with 0.5% Triton X-100 (Sigma-Aldrich, Inc., St. Louis, MO, USA) in PBS. Cells were immunostained with primary antibodies to the C-terminal Myc-DDK tag of the plasmid (1:5000 rat anti-DYKDDDDK tag antibody, 200473; Agilent Technologies) and basal body (1:1000 rabbit anti-pericentrin; Sigma-Aldrich, Dorset, UK); secondarily stained with 1:300 donkey Alexa Fluor 488–conjugated anti-rat (Life Technologies) and 1:300 donkey Alexa Fluor 647–conjugated anti-rabbit (Life Technologies); and mounted with ProLong Gold Antifade Mountant with DAPI (Life Technologies). Cells were imaged with confocal microscopy (Zeiss LSM 700; Carl Zeiss Microscopy, Ltd., Cambridge, UK). The percentage of transfected cells with localization of IFT140 to the basal body was calculated from a mean of three independent experiments with >100 cells counted per experiment (statistical analysis with a one-way analysis of variance and post hoc comparison using a Bonferroni correction; IBM SPSS Statistics version 22, IBM Corporation, New York, USA).

Results

Ophthalmologic and Systemic Findings

Clinical details are summarized in Table 1, with clinical imaging described in Figure 1. All patients had a retinal dystrophy characterized by nyctalopia and progressive field loss, with fundus features and electrophysiology (available in three patients) consistent with RP.

Family 1 of Northern Pakistan origin was comprised of the proband (patient 1.1) and his affected second cousins; two of the three affected second cousins (patients 1.2 and 1.3) were available for clinical examination. Patient 1.1 was born at full term to consanguineous parents. He was noted to have reduced night vision at 2 years of age. Fundus examination demonstrated mild midperipheral retinal changes only (Fig. 1). Electroretinography (ERG) performed at age 8 demonstrated a relatively severe rod-cone dystrophy with marked bilateral macular involvement that had progressed when repeated at age 13 years. Systemically, patient 1.1 was well with no dysmorphic features. At age 13, his height was in the 50th–75th centile, weight in the 75th centile, and head circumference in the 25th centile. His fingers were noted to be long, and he had no skeletal abnormalities. Hand and hip x-rays were normal (Supplementary Fig. S1). He had a history of congenital right pelvico-ureteric junction obstruction and secondary hydronephrosis, which required surgical correction at 4 years of age. Renal and liver function blood tests were normal at age 13 years, and renal ultrasound demonstrated a normal left kidney. On the right, there was global cortical thinning and loss of normal corticomedullary differentiation consistent with the history of hydronephrosis.

Blood samples were obtained from all three affected second cousins of patient 1.1 to confirm segregation (Fig. 2). Assessment and investigation was possible for the two male patients: 1.2 and 1.3. Both developed visual symptoms in childhood with preservation of central vision until their 40s. Both had retinal changes of RP with attenuated vessels, macular atrophy, and midperipheral pigmentary change, which was worse in the older brother. Neither brother had any syndromic features. Specifically, hand x-rays did not demonstrate shortened phalanges, and renal and liver function was normal.

Patient 2, of Caucasian British origin, first noticed nyctalopia at age 16 years, with peripheral field loss noted in his mid-20s when he was diagnosed with RP. Loss of central vision occurred by 50 years of age, with fundus features of a severe and extensive pigmentary retinopathy. There was no history of skeletal or renal abnormalities. A hand x-ray did not identify shortened phalanges, and renal function blood tests were normal at age 67 years (Supplementary Fig. S1). There was a history of progressive hearing loss noted at the age of 4 years, which required hearing aids. Audiometry revealed symmetrical bilateral high-frequency loss and bilateral plateau loss of 25 to 30 db in 250- to 2000-kHz frequencies. The hearing loss was atypical for Usher syndrome. There was no other medical history of note. His younger sister also has RP but without hearing loss. Clinical examination was not possible, but a DNA sample was obtained.

Family 3 is from the Gujarat region of India. The proband, patient 3.1, noted nyctalopia in his late 20s and problems with glare. He noted reduced left vision at age 44 years. Fundus examination revealed extensive pigmentary change and vessel attenuation. An ERG was consistent with severe generalized retinal dysfunction in both eyes. Patient 3.2 presented with nyctalopia and progressive peripheral field loss in her early 30s. When last reviewed at age 57, visual acuity was still good at 0.2 logMAR each eye (Snellen 20/32), despite marked vessel attenuation and generalized atrophy of the posterior pole. Neither patient has any systemic manifestations. Both patients have normal serum creatinine but estimated glomerular filtration rates (GFRs) that are borderline and under review. Both are hypertensive on oral medications. Patient 3.2 has had stable creatinine and GFR over 6 years of monitoring.

Family 4 is from the Punjab region of Pakistan. The proband developed nyctalopia in the early teenage years without any other noticeable symptoms. An ERG was consistent with a severe rod-cone dystrophy. When last reviewed at age 26 years, the patient was systemically well with no clinically apparent syndromic features of disease. Further investigations were unfortunately not possible as the patient is no longer contactable.

Family 5 is British Caucasian. The proband noted difficulty with dark and light adaptation in his late 20s but otherwise remains without symptoms. At last review at age 31 years, the visual acuity was right 0.0 logMAR, left −0.1 logMAR, with mild retinal changes only. He was systemically well, with normal renal function and ultrasound. A skeletal survey was also normal.

Molecular Investigations

In family 1, WES identified a homozygous variant, c.1451C > T(p.Thr484Met), with segregation in five unaffected and three affected family members supporting causality (Table 2; Fig. 2). This variant has been previously reported.[16] No other predicted pathogenic variants were identified in known retinal genes. In family 2, WES identified a splice site variant c.2399+1G > T that has been previously reported in four syndromic patients and a novel missense variant, c.2815T > C (p.Ser939Pro) predicted to be tolerated in silico.[5,6] Patient 2's affected sister also carries both variants, with his son carrying the missense variant only, confirming that the mutations are in *trans*.[5,6]

A targeted gene panel of 176 genes identified an apparent homozygous variant c.998G > A(p.Cys333Tyr) in the third proband. This was also present in two other

Table 1. Summary of Clinical Features

Patient	Age of Onset	Age at Last Review, logMAR Visual Acuity (Snellen), Refractive Error	Key Fundus Findings	Other Findings	ERG, PERG	Serum Creatinine (μmol/L) (70–120)	eGFR, (mL/min/m²) (>90 normal)
1.1 GC 17830	2 years	13 years R 0.0 (6/6) L 0.0 (6/6) R +0.25/−1.25 ×40 L −5.50/−0.50 ×140	Midperipheral hypopigmented dots, mild RPE atrophy	Humphrey visual fields, 24-2: extensive loss of peripheral field, preserved central 10° Ishihara: R and L 17/17	Age 13, residual PERG activity, severe loss of both rod and cone systems	N	N
1.2	First decade	45 years R 0.7 (6/30) L 0.5 (6/19)	Midperipheral RPE hypopigmentary change with intraretinal pigmentary migration, macular atrophy	Early cataract RE L cataract surgery age 44	Not done	N	N
1.3	First decade	44 years R 0.3 (6/12) L 0.3 (6/12)	Midperipheral RPE hypopigmentation, early macular atrophy	Early lens opacity	Not done	N	N
2 GC 1558	16 years	67 years R HM L PL	Posterior pole chorioretinal atrophy, extensive midperipheral pigmentation, severely attenuated vessels	Confrontation visual fields: <5° BE Cataract surgery BE late 40s, myopic prior	Not done	76	95
3.1 GC 4303	Late 20s	53 years R 0.7 (6/30) L 1.8 (1/60)	R cystoid macular edema with epiretinal membrane, B macular atrophy, attenuated vessels extensive pigmentary change	Confrontation visual fields: 20° on R, 10° on L Early cataract	Age 45, undetectable PERG and rod-specific ERG, markedly subnormal cone	115	61
3.2	Early 30s	57 years R 0.2 (6/9.5) L 0.2 (6/9.5)	Marked vessel attenuation with nasally occluded vessels, extensive atrophy particularly of posterior pole, midperipheral pigmentary change	Early cataract BE Ishihara: R 2/17 L 4/17	Not done	91	56
4 GC 20552	14 years	26 years R 0.3 (6/12) L 0.2 (6/9) R −2.50/−0.75 ×15 L −1.75/−1.25 ×10	Bilateral mild epiretinal membrane, mild RPE change in mid-periphery	Early subcapsular cataract Ishihara: R 7/17 L 17/17	Age 25, subnormal PERG, undetectable rod specific responses, subnormal cone	NA	NA
5 GC 21161	28 years	31 years R 0.0 (6/6) L −0.1 (6/4.8)	Attenuated vessels, midperipheral RPE mottling	Confrontation visual fields: full Ishihara: R 17/17 L 17/17	Not done	77	109

eGFR, estimated glomerular filtration rate; GC, genetic family number; N, normal; NA, not available; PERG, pattern electroretinogram.

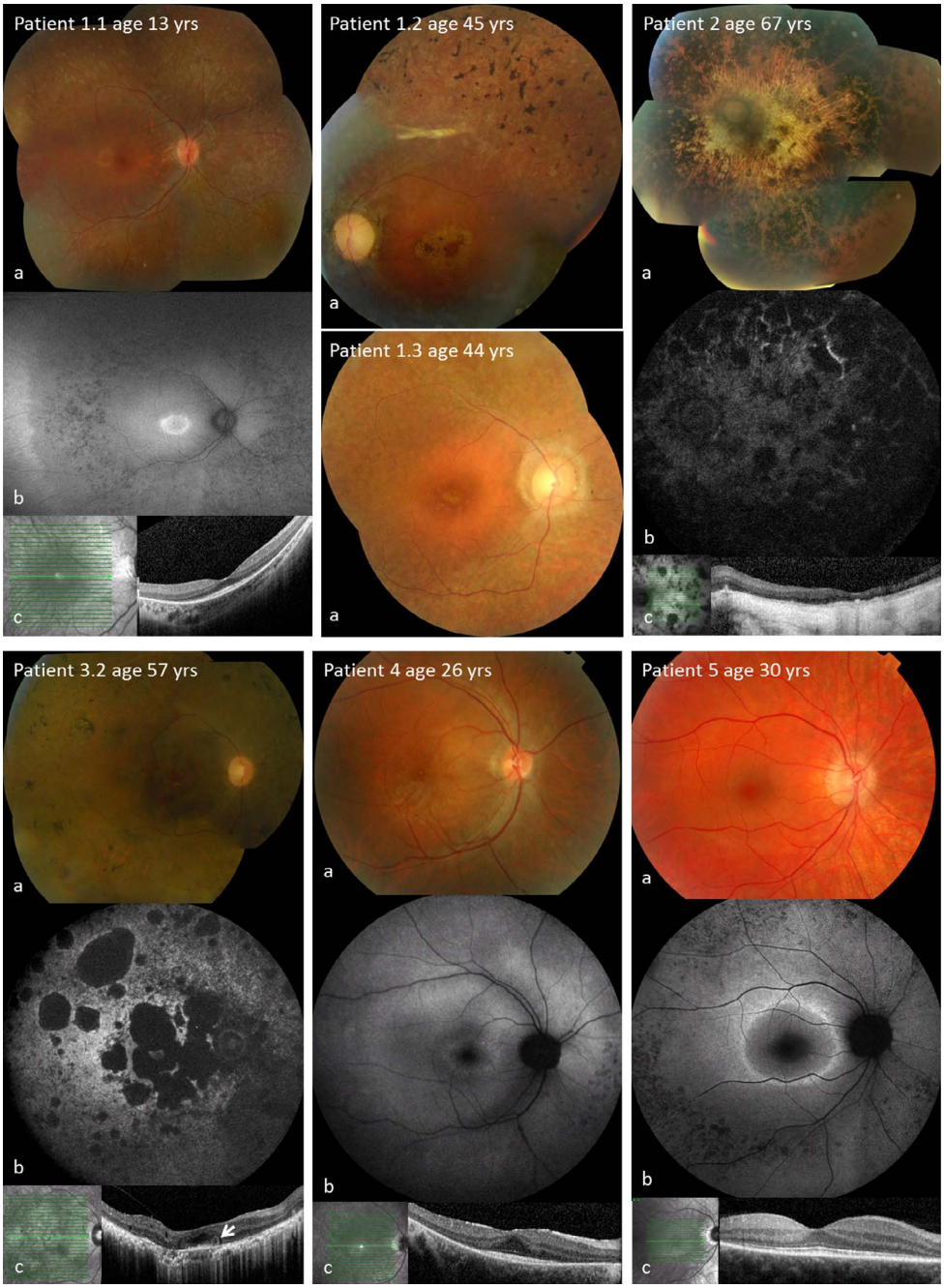

Figure 1. Retinal imaging in *IFT140*-related retinal dystrophy: (**a**) color fundus photographs, (**b**) fundus autofluorescence, and (**c**) optical coherence tomography. Patient 1.1, age 13 years, right eye: (**a**) diffuse, midperipheral white dots with para-foveal early atrophy in the macula (arrow), (**b**) midperipheral reduced autofluorescence in area of white dots with central increased ring of increased autofluorescence in macula, and (**c**) centrally preserved inner segment ellipsoid (ISe) band. Patient 1.2, age 45 years, left eye: (**a**) central macula atrophy with peripheral intraretinal pigmentary migration in regions of depigmentation. Patient 1.3, age 44 years, left eye: (**a**) central macular atrophy with midperipheral hypopigmentary dots. Patient 2, age 67 years, left eye: (**a**) posterior pole atrophy with heavy midperipheral pigmentary change, (**b**) extensive loss of autofluorescence throughout retina, particularly in midperiphery, and (**c**) extensive loss of outer retina and inner choroid. Patient 3.2, age 57 years, right eye: (**a**) macular atrophy, midperipheral RPE atrophy, and pigment change with marked vessel attenuation and vessel occlusion nasally, (**b**) widespread reduced autofluorescence particularly in posterior pole, and (**c**) disorganized retina with loss of outer retina and outer retinal tubulation (*arrow*). Patient 4, age 26 years, right eye: (**a**) mild midperipheral RPE atrophy, (**b**) ring of increased autofluorescence in macula with small dots of reduced autofluorescence nasally, and (**c**) ISe band preserved centrally in region corresponding to the FAF increased ring. Patient 5, age 30 years, right eye: (**a**) attenuated vessels, midperipheral RPE mottling/hypopigmentation, (**b**) ring of increased autofluorescence in the macula, speckled reduction in the midperiphery, and (**c**) ISe band preserved centrally.

affected family members, with one unaffected sibling not harboring the variant; parental DNA was unavailable. It is therefore possible, in this nonconsanguineous family, that the affected patients are hemizygous with a deletion on the other allele. This variant has not been reported in an affected patient before but is present in 2 of 121,370 alleles on ExAC.

WGS identified the same homozygous variant in a fourth unrelated family (patient 4). Affected and unaffected family members overseas were unavailable for further testing.

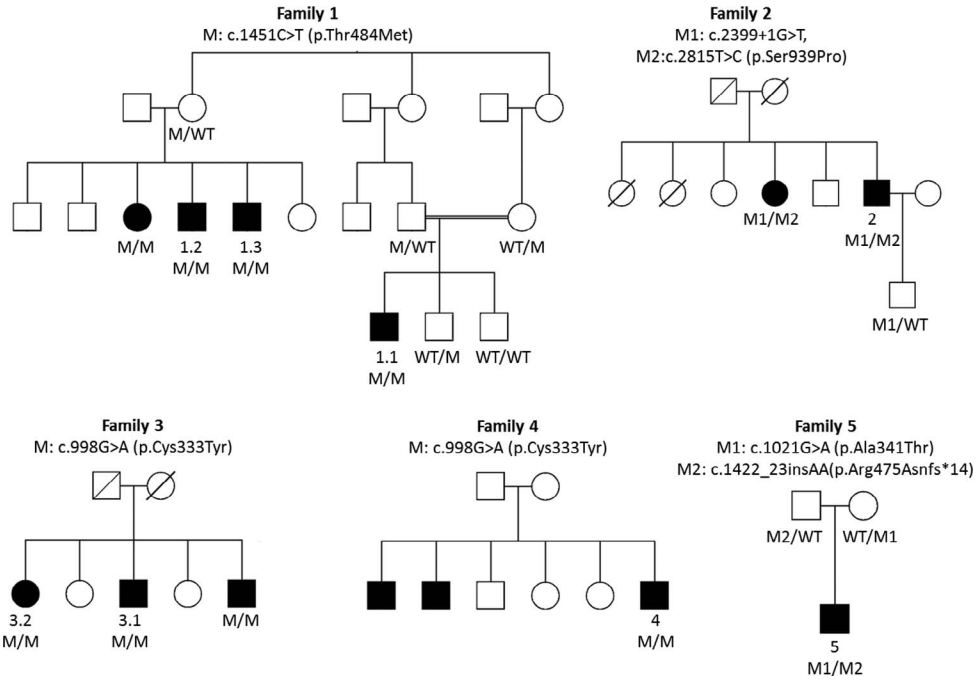

Figure 2. Pedigrees and variant segregation for the five families.

Patient 5 also underwent targeted sequencing of 176 retinal genes, identifying two variants. The first, c.1021G > A (p.Ala341Thr), has an allele frequency of 10 in 119,692 on ExAC and is predicted to be damaging in silico (SIFT 0.03, Polyphen2 1.00). The second is a novel frameshifting mutation, c.1422_1423insAA (p.Arg475Asnfs*14). Segregation in his parents confirmed the mutations to be in *trans*.

Conservation of the missense variants identified in this study was compared to syndromic missense variants across a diverse range of orthologues (Supplementary Fig. S2). Ala341Thr, Thr484Met, and Ser939Pro are not conserved, and Cys333Tyr is fully conserved. Six of nine syndromic missense mutations are fully conserved, and three are not conserved.

Localization of IFT140 and Mutants in hTERT-RPE1 Cells

Site-directed mutagenesis using mutation-specific complementary primer pairs (Supplementary Table S1) generated four plasmid clones. Mutagenesis was confirmed by sequencing of the entire open reading frame. A total of six plasmids were used in cell transfection experiments: two contained nonsyndromic mutations c.1451C > T(p.Thr484Met, T484M) and c.2815T > C (p.Ser939Pro, S939P); one previously unreported mutation, c.1319T > C (p.Leu440Pro, L440P), from a patient with Leber congenital amaurosis and renal failure (Perrault I, written communication, 2015); a previously reported plasmid with a syndromic mutation c.1990G > A (p.Glu664Lys,E664K)[5]; the WT plasmid; and a polymorphism, c.2330T > G (p.Leu777Arg, L777R), rs34535263. Following transient transfection of IFT140 plasmids in hTERT-RPE1 cells and subsequent immunostaining, analysis of aberrant IFT140 localization with the basal body was performed (Fig. 3). Mean transfection efficiency was 38%, with generalized cytoplasmic staining frequently observed. Those cells with specific basal body labeling by IFT140 were counted. Statistically significant aberrant localization was found for T484M, S939P, L440P, and E664K compared with WT and L777R ($P < 0.0001$). No significant difference was found between T484M, S939P, L440P, and E664K ($P = 1$) or between T484M and S939P compared with the syndromic mutants L440P and E664K.

Discussion

This report describes the association of *IFT140* mutations and nonsyndromic retinal dystrophy. A strength of this present study in addition to detailed ophthalmic phenotyping is the

Table 2. Summary of Molecular Results With Predicted Pathogenicity and Previous Reports

Family	Variant	Predicted Effect	Sift Score	Polyphen2 Score	First Report in Patient	ExAC Database Allele Frequency
1	c.1451C > T	p.Thr484Met	0.02	0.980	Xu 2015[16]	5 of 120,980
2	c.2399+1G > T	Abolish strong donor site	—	—	Perrault 2012[5]	4 of 66,732
	c.2815T > C	p.Ser939Pro	0.22	0.155	Novel	Not found
3 and 4	c.998G > A	p.Cys333Tyr	1.00	0.991	Not reported	2 of 121,370
5	c.1021G > A	p.Ala341Thr	0.03	1.000	Not reported	10 of 66,132
	c.1422_23insAA	p.Arg475Asnfs*14	—	—	Novel	Not found

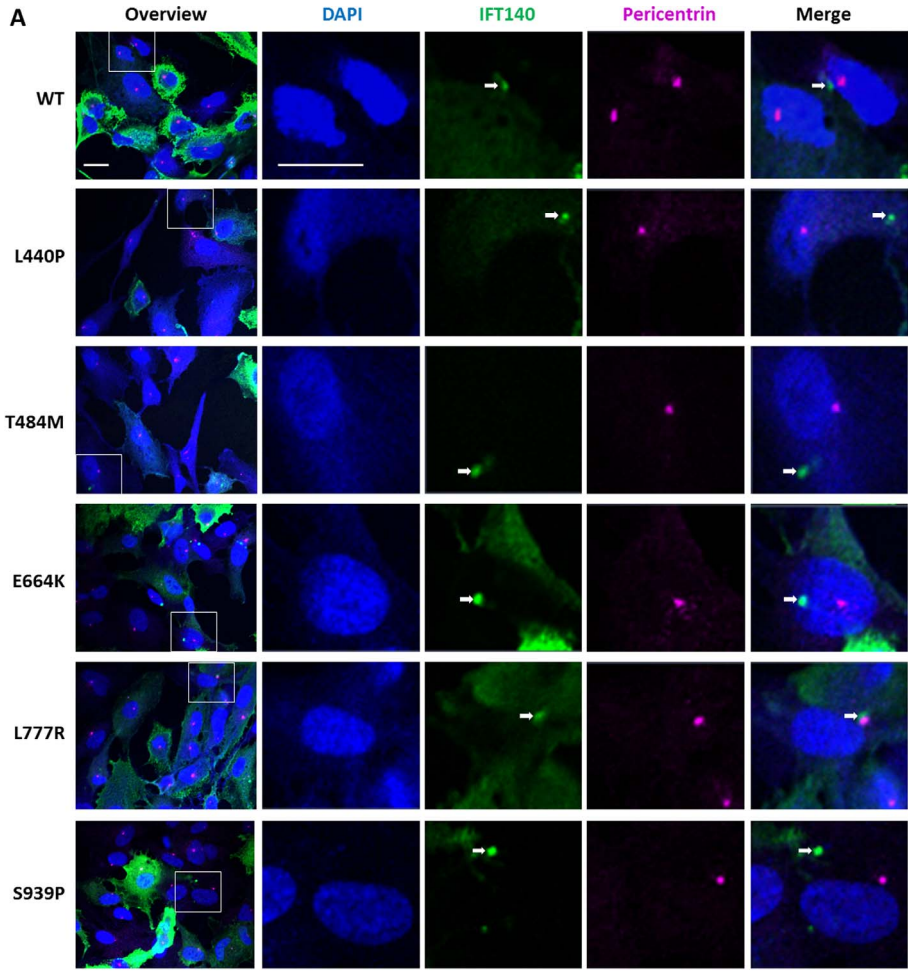

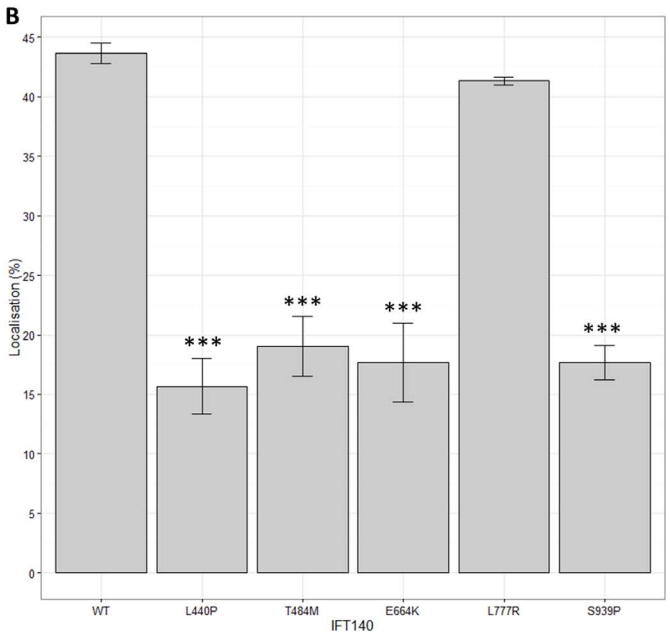

Figure 3. Aberrant localization of IFT140 with basal bodies in transiently transfected hTERT-RPE1 cells. (**A**) Six Myc-DDK–tagged IFT140 plasmid constructs comprising wild type (WT) and five mutants: L440P (syndromic), T484M (nonsyndromic), E664K (syndromic), L777R (polymorphism), and S939P (nonsyndromic). Cells were immunostained with primary antibodies to the IFT140 plasmid (rat anti-DYKDDDDK Tag antibody), and basal body (rabbit anti-pericentrin) and secondarily stained with donkey anti-rat and donkey anti-rabbit. Cells were visualized with Zeiss confocal microscopy. Expressed IFT140 (*white arrow*) and basal body localization were reduced in all mutants compared with WT and a single nucleotide

Investigative Ophthalmology & Visual Science

polymorphism, L777R. *Scale bar.* 20 μm. (**B**) The percentage of transfected cells with localization of IFT140 to the basal body was calculated from a mean of three independent experiments with >100 cells counted per experiment. A statistically significant difference was found between WT and E664K, L440P, T484M, and S939P (***$P < 0.0001$) and between L777R and E664K, L440P, T484M, and S939P ($P < 0.0001$), with no difference between WT and L777R ($P = 1$). There was also no statistically significant difference found between the syndromic mutants, E664K and L440P, and the T484M and S939P mutants ($P = 1$).

systemic investigation of all but one patient, as well as including five patients in their fifth to seventh decades, which is far older than any previously reported patients. The patients have typical features of RP presenting from early childhood to the fourth decade, and all are developmentally normal, with no apparent skeletal or neurological abnormalities. Cone-shaped epiphyses are universally found prepubertally in *IFT140*-related syndromic disease. This abnormality is not apparent in adults, although shortening of the phalanges can still be detected.[30] Prepubertal hand and pelvic x-rays in patient 1.1 were normal. In patients 1.2, 1.3, 2, and 5, hand x-rays did not identify shortened phalanges, but it remains possible that x-rays during childhood could have revealed evidence of the cone shape abnormality. Seven of eight patients were available for renal investigations. Renal function was normal except for patients 3.1 and 3.2, with borderline renal function at age 53 and 57 years, respectively. It is possible that this mild renal impairment is related to *IFT140*, but given their age and hypertension, it may be unrelated. Patient 1.1 had a unilateral congenital pelvico-ureteric obstruction surgically repaired. This abnormality has not been reported in *IFT140*-related disease, and the other kidney is structurally normal on ultrasound; it is likely that this is an incidental finding. His two older affected second cousins have normal renal function in their 40s.

All but one of the previously reported syndromic patients with *IFT140* mutations had a severe, early-onset retinal dystrophy and undetectable or severely attenuated ERG.[5–7] The exception, a patient homozygous for c.699T > G (p.Ile233Met), had no evidence of retinal dystrophy at age 2 years but did have skeletal and renal manifestations.[5] Of seven patients recently reported with isolated retinal dystrophy due to *IFT140,* five have RP with onset of nyctalopia ranging from 7 to 33 years old, and two have severe early-onset retinal dystrophy.[15] There was no evidence of renal or skeletal involvement, but one patient had hypogonadism and fatty liver, which have been reported in other ciliopathies. It was not clear if all patients underwent systemic investigation and renal function. A further report of 12 patients focused on the ophthalmic phenotype, describing it as severe with infantile onset, hyperopia, and flat ERG (age, <2–20 years). The patients reported in this present study have milder and later onset retinal dystrophy than the majority of those previously reported with fundus features consistent with RP. Refraction, available in two patients, was myopic.

All reported patients with syndromic forms of *IFT140*-related ciliopathy have developed end-stage renal failure by their second decade, with the exception of 10 families homozygous for p.Glu664Lys (reported ages, 10 months to 17 years).[5–7,16] The affected children in these families presented in infancy with severe early-onset retinal dystrophy consistent with a diagnosis of Leber congenital amaurosis and with additional syndromic findings including epilepsy, hypotonia, and developmental delay. In all patients in whom hand x-rays were performed, cone-shaped epiphyses were identified. Systemic investigations were unavailable for four families.[16] The lack of overt renal dysfunction suggests a possible genotype–phenotype correlation for this specific mutation.[5,7,16] However, there has been one reported patient homozygous for this variant, with renal failure and kidney transplant age at 17 years, raising the possibility that renal dysfunction may still occur with this allele but perhaps later than with other syndromic disease alleles.[16]

Phenotypic heterogeneity of several ciliopathy genes has been well established, including *CEP290*, *IQCB1, IFT172*, *BBS1*, and *BBS3*.[13,14,31–33] In the case of *CEP290*, there is evidence for a dosage-dependent phenotype with bi-allelic loss of function mutations associated with Joubert syndrome and the common c.2991+1655A > G splicing mutation, in which a small amount of protein is still produced, associated with Leber congenital amaurosis.[13] In addition, *CEP290* mutations in functionally critical regions, despite predicted residual protein production, were associated with a more severe phenotype.[34] Three nonsyndromic families in this report have bi-allelic missense variants, as do several of the previously reported syndromic families (Supplementary Table S2).[5–7] This would suggest that phenotypic variability is not related to the type of mutation. Only one patient with bi-allelic premature termination codons has been reported, which may indicate an essential developmental role for IFT140.[16] Mice homozygous for *Ift140*$^{-/-}$ die midgestation, indicating embryonic lethality for a null phenotype.[35]

IFT140 is a 1462-amino-acid protein encoded by 31 exons and consists of two types of domain; five WD repeats and nine tetratricopeptide repeats.[36] Reported mutations arise throughout the gene with no clustering or domain preference. Of the four missense variants in this report, p.Cys333Tyr and p.Ala341Thr arise within the WD5 domain but the other two are not located within known functional domains. Of the previously reported syndromic mutations, two arise within functional domains (p.Val292Met and p.Tyr311Cys in WD4) and the remaining seven do not. Conservation of missense amino acid residues in orthologues demonstrates a lack of conservation of three of the nonsyndromic residues, with one fully conserved. Three of nine syndromic mutations are not conserved, precluding any conclusion (Supplementary Fig. S2). The Cys333Tyr allele was identified in two families, and it would suggest that this may be a retina-specific allele. The variant Thr484Met was recently identified in conjunction with a second missense variant in a patient with nonsyndromic Leber congenital amaurosis, indicating that this allele may also be retina specific. The nonconserved Ala341Thr variant was identified in a patient with a novel frameshifting variant, which has not been reported in an affected patient before. The nonconserved Ser939Pro residue is predicted to be tolerated in silico and arises in conjunction with a splice site variant previously reported in syndromic disease. These results may indicate that the Ala341Thr and Ser939Pro variants are less deleterious to protein function such that there is a nonsyndromic manifestation of disease.

Transient expression of IFT140 in hTERT-RPE1 cells transfected with a Myc-DDK–tagged IFT140 plasmid demonstrates localization of IFT140 with the basal body. This was significantly reduced in mutant cells compared with WT and L777R cells ($P < 0.0001$). No difference was found between the two missense variants from families in this report and the two reported syndromic missense variants, indicating a deleterious effect on protein trafficking in vitro for all mutants studied. This supports causality of these two nonsyndromic missense variants in vitro.

In this report, five families with apparently isolated RP due to *IFT140* mutations are characterized. Given the potential for systemic complications, children with apparently isolated retinal dystrophy due to *IFT140* mutations may need long-term systemic investigation and renal function monitoring. However, it is likely that some patients will have lifelong isolated retinal disease, and as more patients are reported, specific allele phenotypes may emerge.

Acknowledgments

The authors thank Sophie Saunier and Albane Bizet for the technical help with the cell transfection studies and the gift of the pCMV-IFT140-Myc-DDK and pCMV-IFT140-E664K-Myc-DDK plasmids.

Supported by the National Institute for Health Research England (NIHR) for supporting the NIHR BioResource–Rare Diseases (RG65966) and the Biomedical Research Centres at Moorfields Eye Hospital and the UCL Institute of Ophthalmology (BRC2_003) and at the Manchester Biomedical Research Centre; The Foundation Fighting Blindness (C-CL:0710-0505-MEH10-02); Fight For Sight (1318 and 1801); Moorfields Eye Hospital Special Trustees (ST1109B); Rosetrees Trust (M184); RP Fighting Blindness (GR581); La Fondation pour la Recherche Médicale; The Institut National de la Santé et de la Recherche Médicale; The Imagine Institute; and The Association Retina France and Programme Hospitalier pour la Recherche Clinique (AOM 09058).

Disclosure: **S. Hull**, None; **N. Owen**, None; **F. Islam**, None; **D. Tracey-White**, None; **V. Plagnol**, None; **G.E. Holder**, None; **M. Michaelides**, None; **K. Carss**, None; **F.L. Raymond**, None; **J-M. Rozet**, None; **S.C. Ramsden**, None; **G.C.M. Black**, None; **I. Perrault**, None; **A. Sarkar**, None; **M. Moosajee**, None; **A.R. Webster**, None; **G. Arno**, None; **A.T. Moore**, Sanofi (S), Oxford Biomedica (S), Sucampo Pharmaceuticals (S)

References

1. Tsujikawa M, Malicki J. Intraflagellar transport genes are essential for differentiation and survival of vertebrate sensory neurons. *Neuron*. 2004;42:703–716.
2. Crouse JA, Lopes VS, Sanagustin JT, Keady BT, Williams DS, Pazour GJ. Distinct functions for IFT140 and IFT20 in opsin transport. *Cytoskeleton (Hoboken)*. 2014;71:302–310.
3. Mukhopadhyay S, Wen X, Chih B, et al. TULP3 bridges the IFT-A complex and membrane phosphoinositides to promote trafficking of G protein-coupled receptors into primary cilia. *Genes Dev*. 2010;24:2180–2193.
4. Wei Q, Zhang Y, Li Y, Zhang Q, Ling K, Hu J. The BBSome controls IFT assembly and turnaround in cilia. *Nat Cell Biol*. 2012;14:950–957.
5. Perrault I, Saunier S, Hanein S, et al. Mainzer-Saldino syndrome is a ciliopathy caused by IFT140 mutations. *Am J Hum Genet*. 2012;90:864–870.
6. Schmidts M, Frank V, Eisenberger T, et al. Combined NGS approaches identify mutations in the intraflagellar transport gene IFT140 in skeletal ciliopathies with early progressive kidney Disease. *Hum Mutat*. 2013;34:714–724.
7. Khan AO, Bolz HJ, Bergmann C. Early-onset severe retinal dystrophy as the initial presentation of IFT140-related skeletal ciliopathy. *J AAPOS*. 2014;18:203–205.
8. Mainzer F, Saldino RM, Ozonoff MB, Minagi H. Familial nephropathy associated with retinitis pigmentosa, cerebellar ataxia and skeletal abnormalities. *Am J Med*. 1970;49:556–562.
9. Bertelsen M, Jensen H, Bregnhøj JF, Rosenberg T. Prevalence of generalized retinal dystrophy in Denmark. *Ophthalmic Epidemiol*. 2014;21:217–223.
10. Hartong DT, Berson EL, Dryja TP. Retinitis pigmentosa. *Lancet*. 2006;368:1795–1809.
11. Xu Y, Guan L, Shen T, et al. Mutations of 60 known causative genes in 157 families with retinitis pigmentosa based on exome sequencing. *Hum Genet*. 2014;133(10):1255–1271.
12. Littink KW, van den Born LI, Koenekoop RK, et al. Mutations in the EYS gene account for approximately 5% of autosomal recessive retinitis pigmentosa and cause a fairly homogeneous phenotype. *Ophthalmology*. 2010;117:2026–2033.
13. den Hollander AI, Koenekoop RK, Yzer S, et al. Mutations in the CEP290 (NPHP6) gene are a frequent cause of Leber congenital amaurosis. *Am J Hum Genet*. 2006;79:556–561.
14. Estrada-Cuzcano A, Koenekoop RK, Senechal A, et al. BBS1 mutations in a wide spectrum of phenotypes ranging from nonsyndromic retinitis pigmentosa to Bardet-Biedl syndrome. *Arch Ophthalmol*. 2012;130:1425–1432.
15. Xu M, Yang L, Wang F, et al. Mutations in human IFT140 cause non-syndromic retinal degeneration. *Hum Genet*. 2015;134(10):1069–1078.
16. Bifari IN, Elkhamary SM, Bolz HJ, Khan AO. The ophthalmic phenotype of IFT140-related ciliopathy ranges from isolated to syndromic congenital retinal dystrophy [published online ahead of print September 10, 2015]. *Br J Ophthalmol*. doi:10.1136/bjophthalmol-2015-307555.
17. Bach M, Brigell MG, Hawlina M, et al. ISCEV standard for clinical pattern electroretinography (PERG): 2012 update. *Doc Ophthalmol*. 2013;126:1–7.
18. Marmor MF, Fulton AB, Holder GE, et al. ISCEV standard for full-field clinical electroretinography (2008 update). *Doc Ophthalmol*. 2009;118:69–77.
19. Zernant J, Külm M, Dharmaraj S, et al. Genotyping microarray (disease chip) for Leber congenital amaurosis: detection of modifier alleles. *Invest Ophthalmol Vis Sci*. 2005;46:3052–3059.
20. Le Quesne Stabej P, Saihan Z, Rangesh N, et al. Comprehensive sequence analysis of nine Usher syndrome genes in the UK National Collaborative Usher Study. *J Med Genet*. 2012;49:27–36.
21. Li H, Durbin R. Fast and accurate short read alignment with Burrows-Wheeler transform. *Bioinformatics*. 2009;25:1754–1760.
22. McKenna A, Hanna M, Banks E, et al. The Genome Analysis Toolkit: A MapReduce framework for analyzing next-generation DNA sequencing data. *Genome Res*. 2010;20:1297–1303.
23. Raczy C, Petrovski R, Saunders CT, et al. Isaac: Ultra-fast whole-genome secondary analysis on Illumina sequencing platforms. *Bioinformatics*. 2013;29:2041–2043.
24. Abecasis GR, Altshuler D, Auton A, et al. A map of human genome variation from population-scale sequencing. *Nature*. 2010;467:1061–1073.
25. Adzhubei IA, Schmidt S, Peshkin L, et al. A method and server for predicting damaging missense mutations. *Nat Methods*. 2010;7:248–249.
26. Kumar P, Henikoff S, Ng PC. Predicting the effects of coding non-synonymous variants on protein function using the SIFT algorithm. *Nat Protoc*. 2009;4:1073–1081.
27. McWilliam H, Li W, Uludag M, et al. Analysis Tool Web Services from the EMBL-EBI. *Nucleic Acids Res*. 2013;41:W597–W600.
28. Flicek P, Amode MR, Barrell D, et al. Ensembl 2014. *Nucleic Acids Res*. 2014;42:D749–D755.
29. Reese MG, Eeckman FH, Kulp D, Haussler D. Improved splice site detection in Genie. *J Comput Biol*. 1997;4:311–323.
30. Beals RK, Weleber RG. Conorenal dysplasia: a syndrome of cone-shaped epiphysis, renal disease in childhood, retinitis pigmentosa and abnormality of the proximal femur. *Am J Med Genet A*. 2007;143A:2444–2447.
31. Estrada-Cuzcano A, Koenekoop RK, Coppieters F, et al. IQCB1 mutations in patients with leber congenital amaurosis. *Invest Ophthalmol Vis Sci*. 2011;52:834–839.

32. Bujakowska KM, Zhang Q, Siemiatkowska AM, et al. Mutations in IFT172 cause isolated retinal degeneration and Bardet-Biedl syndrome. *Hum Mol Genet*. 2015;24:230–242.

33. Abu Safieh L, Aldahmesh MA, Shamseldin H, et al. Clinical and molecular characterisation of Bardet-Biedl syndrome in consanguineous populations: the power of homozygosity mapping. *J Med Genet*. 2010;47:236–241.

34. Drivas TG, Wojno AP, Tucker BA, Stone EM, Bennett J. Basal exon skipping and genetic pleiotropy: a predictive model of disease pathogenesis. *Sci Transl Med*. 2015;7:291ra297.

35. Miller KA, Ah-Cann CJ. Welfare MF, et al. Cauli: a mouse strain with an Ift140 mutation that results in a skeletal ciliopathy modelling Jeune syndrome. *PLoS Genet*. 2013;9:e1003746.

36. UniProt Consortium. UniProt: a hub for protein information. *Nucleic Acids Res*. 2015;43:D204–212.

Investigative Ophthalmology & Visual Science